ACS OMEGA

Open Access

http://pubs.acs.org/journal/acsodf

Article

Removal of Antibiotics from Swine Wastewater Using an Environmentally Friendly Biochar: Performance and Mechanisms

Jessica de Oliveira Demarco,* Stacy L. Hutchinson, Prathap Parameswaran, Ganga Hettiarachchi, and Trisha Moore

Cite This: https://doi.org/10.1021/acsomega.4c07266

Read Online

ACCESS | Metrics & More | Article Recommendations | Supporting Information

ABSTRACT: Antibiotics used in the swine industry to treat diseases and improve animal growth are poorly absorbed by swine and have been classified as micropollutants due to their occurrence in surface water, wastewater, and soil. This study investigated the capacity of biochar produced from eastern red cedar to remove target antibiotics that have been extensively used in the swine industry. Biochar was produced by pyrolysis from eastern red cedar at 450 °C. The sorption tests were performed by mixing biochar and a solution (1:10 ratio) containing each antibiotic in 100, 300, 600, and 900 $\mu g\ L^{-1}$ concentrations. The results indicate that red cedar biochar was able to effectively remove up to 99.93% tetracycline, 96.23% oxytetracycline, 98.28% chlortetracycline, 76.4% sulfadiazine, and 78.6% sulfamethazine at the lowest concentrations. The removal efficiencies at higher concentrations declined up to 83.52, 47.23, 64.16, 69.8, and 58.4% for tetracycline, oxytetracycline, chlortetracycline, sulfadiazine, and sulfamethazine, respectively. The biochar exhibited stronger adsorption capacity for chlortetracycline and sulfamethazine compared to the other antibiotics. The likely adsorption mechanisms driving the removal of tetracyclines and sulfonamides are hydrogen-bonding and $\pi-\pi$ electron-donor−acceptor, supported by FTIR analyses of the biochar itself. Overall, the results highlighted the potential utilization of eastern red cedar biochar for practical applications, mitigating antibiotic residues from swine wastewater in a cost-effective and environmentally friendly manner due to its relatively low pyrolysis temperature (450 °C) and sustainable repurposing of an invasive tree species.

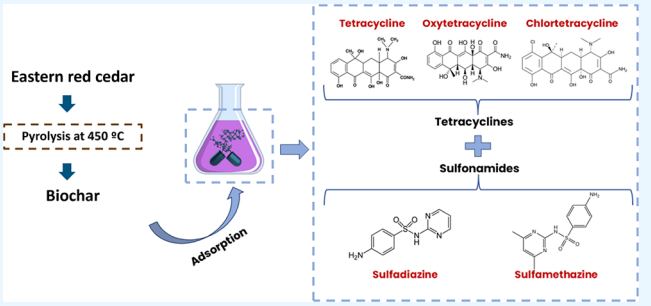

INTRODUCTION

The swine industry is among the top users of antibiotics in the animal industry and uses antibiotics widely to treat, prevent, and control the diseases caused by bacterial infections and hence improve the growth of pigs.[1,2] Due to the overdosage and low assimilation by animals, most antibiotics (70−90%) are excreted into the environment through liquid manure and feces, threatening the health of humans and other organisms by inducing the prevalence of antibiotic-resistant genes in pathogenic bacteria.[3,4] Several antibiotics have been identified in different environmental compartments, such as livestock farms, river water and sediment, soils, and groundwater.[5]

Sulfonamides and tetracyclines are two classes of antibiotics most common in swine wastewater, frequently detected at concentrations of up to 710 and 1000 $\mu g\ L^{-1}$, respectively.[6,7,8] Li et al.[9] investigated the concentrations of 10 commonly used veterinary antibiotics in samples of treated slurries and groundwater to understand the effect of swine feedlot as sources on the groundwater quality downstream. They concluded that all types of antibiotics were detected in either discharged wastewater or groundwater samples; however, tetracyclines and sulfonamides were detected in high concentration and frequency in the wastewater samples. The mean concentrations of tetracyclines and sulfonamides were 416 and 442 $\mu g\ L^{-1}$ in wastewater samples.[9] Thus, there is a need for cost-effective wastewater treatment techniques to remove antibiotics in animal waste, thereby protecting human health and the environment.[10]

Different treatment technologies including biological, physical, chemical, or a combination of these techniques have been employed to treat wastewaters to comply with allowable effluent discharge limits.[11] Biological approaches to treat swine wastewater have focused on anaerobic fermentation, biofilm reactors, sequentially combined aerobic and anaerobic batch reactors (SBR), and denitrification in constructed wetlands. In contrast, physical and chemical methods have emphasized on recovering nitrogen and phosphorus based on precipitation and adsorption mechanisms.[11] Biochar, for example, is an excellent biomass-derived

Received: August 20, 2024
Revised: December 28, 2024
Accepted: January 23, 2025

carbonaceous sorbent for organic contaminants due to its pore structures and surface characteristics that can be applied to treat swine wastewater in combination with other treatment technologies such as anaerobic digestion.[12] Antibiotic removal by biochar adsorption has several advantages, including the use of locally available adsorbent materials, high efficiency (>90%) and selectivity due to its polar functional groups effective in the sorption of polar compounds, and cost-effectiveness when compared to other treatment techniques such as advanced oxidation processes, membrane filtration, and activated carbon adsorption.[13,14]

Additionally, biochar production can contribute to waste management and carbon sequestration efforts by converting organic waste into a beneficial product.[15] These carbonaceous materials are produced through pyrolysis of organic materials, such as plant residue, agricultural waste, or wood chips at high temperatures (usually ≤800 °C).[16,17] For instance, Zhang et al.[6] found that biochar derived from corn straw pyrolyzed at 600 °C had the highest adsorption capacity for tetracycline removal in soil when compared to temperatures ranging from 100 to 600 °C. Similarly, Hu et al.[18] demonstrated effectiveness in removing sulfonamides from water using an attapulgite-modified rice straw biochar pyrolyzed at 700 °C. However, when high pyrolysis temperatures are used, the use of biochar is not feasible for practical applications due to the high costs associated with their production (i.e., high energy requirements for high pyrolysis temperatures) and surface modification.[17]

Pyrolysis is the most costly stage when producing biochar, accounting for 36% of the total production cost due to the consumption of large amounts of energy.[19] The pyrolysis process also generates bio-oil, a liquid coproduct that may be used to generate energy or as feedstock to generate chemicals.[20] Therefore, reducing the energy requirements for biochar production would improve its economic feasibility for large-scale application.[21] Another crucial factor in the widespread production and commercialization of biochar is the identification of abundant, sustainable, and readily available feedstock options that have significant environmental and economic implications.[22]

The objective of this study, therefore, was to investigate the capacity of eastern red cedar biochar pyrolyzed at a relatively low temperature of 450 °C to remove tetracycline and sulfonamide antibiotics. Specifically, the adsorption mechanisms of three tetracyclines (tetracycline, oxytetracycline, and chlortetracycline) and two sulfonamides (sulfadiazine and sulfamethazine) at different concentrations were investigated.

Eastern red cedar is native to the eastern United States and southern Canada but is considered an invasive species in areas of the Great Plains where it is displacing ideal native grass species.[23] Unfortunately, eastern red cedar rapid expansion into grassland prairies has led to several environmental problems, including greater wildfire risk, reduced water yield, unfavorable wildlife habitat, changes in nutrient cycling and carbon sequestration, and reduced forage.[24] Biochar produced from hardwood was found to have high porosity and thus may be effective in absorbing large amounts of organic chemicals.[25] However, there is a lack of research regarding the adsorption of antibiotics using biochar derived from eastern red cedar (*Juniperus virginiana* L.), which is a softwood tree. This research offers unique contributions by demonstrating the novel use of eastern red cedar biochar for removing antibiotics from swine wastewater, providing insights into the adsorption mechanisms at lower pyrolysis temperatures and highlighting practical implications for sustainable wastewater treatment in agricultural settings.

MATERIALS AND METHODS

Chemicals and Materials. Tetracycline hydrochloride (CAS: 64-75-5, $C_{22}H_{24}N_2O_8$·HCl), oxytetracycline hydrochloride (CAS: 2058-46-0, $C_{22}H_{24}N_2O_9$·HCl), chlortetracycline hydrochloride (CAS: 64-72-2, $C_{22}H_{23}ClN_2O_8$·HCl), sulfadiazine (CAS: 68-35-9, $C_{10}H_{10}N_4O_2S$), and sulfamethazine (CAS: 57-68-1, $C_{12}H_{14}N_4O_2S$) were purchased from Sigma-Aldrich. Eastern red cedar biochar was obtained from Blue Earth LLC, located in Manhattan, Kansas, USA. Biochar was produced by pyrolysis from eastern red cedar at 450 °C. The pyrolyzed biochar was ground and passed through a sieve of <595 μm.

Characterization of Biochar. The biochar was produced using all the parts of the eastern red cedar (stem, leaves, and branches). The surface morphology and elemental composition of the eastern red cedar biochar were determined using a scanning electron microscope (SEM) (Nova NanoSEM 450, FEI, USA) with an integrated energy dispersive X-ray spectroscopy analysis (EDS) (X-Max 20 mm^2, Oxford, United Kingdom) silicon-drift detector located at the Electron Nanoscopy Instrumentation Facility, University of Nebraska, Lincoln, USA, with a working voltage of 15 kV.

Fourier transform infrared spectroscopy (FTIR) was performed to identify the main chemical groups on biochar using the Thermo iS-50 FTIR spectrometer (Thermo Fisher Scientific, USA) in the range 450−4000 cm^{-1} with a diamond attenuated reflectance.

The elemental analysis was done using a 2400 Series II CHNS/O Elemental Analyzer (PerkinElmer, USA). The mineral phases and crystal structure of the biochar were identified by means of an EMPYREAN X-ray diffractometer (XRD) (PANanalytical, Netherlands) at a scanning rate of 10°/min from 0 to 90° (2-theta).

The specific surface area, pore volume, and pore size distribution of the biochar were measured from N_2 adsorption−desorption isotherms at 77 K using a surface area analyzer (ASAP 2460, Micrometrics, USA). The surface area (S_{BET}) was calculated by the Brunnauer−Emmett−Teller (BET) method.

Adsorption Experiments. Sorption tests were performed to evaluate the removal of tetracycline, oxytetracycline, chlortetracycline, sulfadiazine, and sulfamethazine, both individually and as a mixture, from an aqueous solution. Sorption tests were performed in quadruplicate. Two milligrams of biochar was dispersed in a scintillation vial with screw caps containing 20 mL of deionized water with a known concentration of each antibiotic (100, 300, 600, and 900 μg L^{-1}). Combinations of antibiotics were prepared to evaluate if the biochar would preferentially sorb certain antibiotics: tetracyclines (tetracycline, oxytetracycline, and chlortetracycline) and sulfonamides (sulfadiazine and sulfamethazine) were both mixed separately to yield separate mixtures, with the same final concentrations each (100, 300, 600, or 900 μg L^{-1}). Then, all tetracyclines and sulfonamides were combined at concentrations of 600 and 300 μg L^{-1}, respectively. Concentrations for tetracyclines and sulfonamides ranging from 100 to 1000 μg L^{-1} can be found in the literature for swine and other livestock and can vary depending on the specific antibiotic, the dosing regimen, and the intended

https://doi.org/10.1021/acsomega.4c07266
ACS Omega XXXX, XXX, XXX−XXX

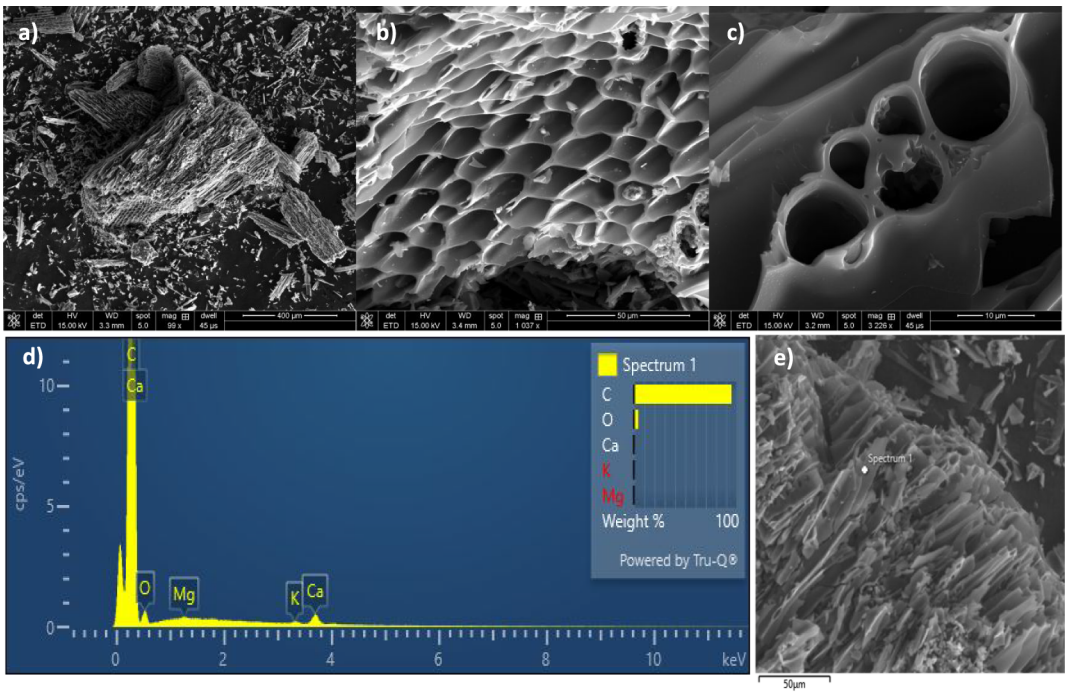

Figure 1. SEM images of eastern red cedar biochar 400 μm (a), 50 μm (b), 10 μm (c), and energy dispersive X-ray spectroscopy analysis (EDS) (d) from the eastern red cedar biochar surface (e).

purpose, such as disease prevention and treatment of infection.[26,27,28]

Sodium hydroxide and HCl solutions (0.01−1 M) were used to change the pH of the solution containing antibiotics to 7. For the majority of adsorbents, the adsorption affinity is favorable within a limited range of solution pH or the adsorption decreases with the increase in the negative surfaces of the sorbents with increasing pH, since acidic functional groups become more negative due to deprotonation.[29]

Samples were placed in a thermostatic oscillator at 150 rpm for 24 h of contact time at room temperature (25 °C) to achieve adsorption equilibrium. The residual antibiotics were analyzed in 0.22 μm filtered samples by a high-performance liquid chromatography (HPLC) system (Waters Acquity HPLC System with a Xevo TQ-S Mass Spectrometer).

The amount of antibiotic adsorbed on biochar (Q_e, mg/g) was calculated from the difference in concentration between the initial (C_0, mg/L) and the equilibrium (C_e, mg/L) solutions (eq 1).

$$Q_e = \frac{C_o - C_e}{m} \times \frac{V}{1000} \quad (1)$$

where V (mL) is the volume of the antibiotic solution and m (g) is the weight of the biochar used.

Adsorption Isotherm Models. In order to better understand the adsorption process, Langmuir and Freundlich adsorption isotherm models were utilized to fit the experimental data. The Langmuir model (eq 2) hypothesizes that a monolayer or shorter adsorption process is proportional to the homogeneous energy on the surface sites:[30]

$$q_e = \frac{bq_{max}C_e}{1 + bC_e} \quad (2)$$

The Freundlich model (eq 3) describes multilayer adsorption on a heterogeneous adsorbent surface:[30]

$$q_e = K_F C_e^{1/n} \quad (3)$$

where q_e (mg g^{-1}) and C_e (mg L^{-1}) are the equilibrium adsorption capacity and concentration, respectively; q_{max} (mg g^{-1}) denotes the maximum adsorption capacity; b (L mg^{-1}) refers to the Langmuir model parameters; and K_F and n are the Freundlich model parameters.

Statistical Analysis. Statistical analyses were performed in R statistical software.[31] One-way ANOVA and Fisher's LSD test were used to assess statistically significant differences ($p < 0.05$) among the antibiotic concentrations.

RESULTS AND DISCUSSION

Biochar Characterization. The surface morphology and chemical composition of the biochar were determined by using SEM and EDS (Figure 1). According to SEM images in Figure 1a,b, eastern red cedar biochar had an irregular surface with a wide range of pore openings. The biochar surface was smooth, containing rod-like structures and pores (Figure 1c). Previous research demonstrated that the microporous structure and high surface area of biochar would provide more adsorption sites for adsorbate.[32] The EDS indicated traces of elements, such as magnesium (Mg), potassium (K), and calcium (Ca) on the biochar surface (Figure 1d). These minerals were distributed across the surface (Figure 1e) and the Mg, K, and Ca contents were found to be 16.76, 12.29, and 70.95%, respectively. Sharma and Ratner[33] compared the mineral composition of wood biochar from previous studies using surface area analysis and concluded that most studies indicated the presence of these minerals next to porous regions. The presence of these Mg, K, and Ca can be a result of the pyrolysis process.[33]

The results of the physicochemical characteristics of eastern red cedar biochar showed that the surface of biochar is mainly composed of carbon (C), oxygen (O), and Ca (Table 1). A high C content was exhibited in the biochar, which can be

https://doi.org/10.1021/acsomega.4c07266
ACS Omega XXXX, XXX, XXX−XXX

Table 1. Physicochemical Characteristics of Eastern Red Cedar Biochar

Element analysis (wt %)									
C	O	H	N	Na	Mg	Si	Ca	K	P
70.1	14.5	2.3	0.6	0.2	2.4	0.7	6.1	0.6	1.8
S_{BET} (m^2 g^{-1})		S_{mic} (m^2 g^{-1})[a]		V_{TOT} (cm^3 g^{-1})[b]		V_{mic} (cm^3 g^{-1})[c]		D_{av} (nm)[d]	
262.13		203.92		0.1528		0.1060		2.33	

[a]Micropore surface area calculated using the *t*-plot method. [b]Total pore volume. [c]Micropore volume calculated with the *t*-plot method. [d]Average pore diameter.

explained by the biochar preparation temperature (450 °C). As can be seen in Table 1, at 450 °C, the carbon content in biochar is relatively high due to the thermal breakdown of organic matter, resulting in a material rich in carbon. Typically, a high pyrolysis temperature can lead to a greater level of carbonization and the formation of more aromatic structures, which are associated with the dehydration and condensation reactions. This process removes volatile compounds and leads to a concentrated carbonaceous residue with aromatic carbon bonds.[34,35] As previously indicated by Yargicoglu et al.,[35] biochars with higher ratios of carbon to nitrogen (C:N) and lower ratios of hydrogen to carbon (H:C) are more likely to have experienced significant thermal alterations due to the greater loss of hydrogen and nitrogen relative to carbon, which can be observed in the eastern red cedar biochar. The eastern red cedar biochar had a BET specific surface area of 262.13 m^2 g^{-1}, a total pore volume of 0.1060 cm^3 g^{-1}, and an average pore size of 2.33 nm. Liu et al.[36] found similar results in their evaluation of the surface characteristics of biochar from cedar sawdust pyrolyzed at temperatures between 450 and 600 °C. They reported a surface area ranging from 250 to 300 m^2 g^{-1}, a pore volume between 0.15 and 0.17 cm^3 g^{-1}, and an average pore size between 2.16 and 2.42 nm. Several authors have noted that the surface area and pore volumes of biochar increase with higher pyrolysis temperatures.[23,37,38] For instance, Vaughn et al.[23] produced eastern red cedar biochar using pyrolysis temperatures from 780 to 850 °C and obtained a surface area of 490 m^2 g^{-1}.

Figure 2 presents the FTIR spectra and XRD analysis of eastern red cedar biochar. The cracking of aliphatic groups, such as methyl, methylene, and methoxyl, and reformation of other functional groups such as carbonyl and carboxyl occur with a temperature around 400 °C.[39] The aromatic groups in the eastern red cedar biochar sample give rise to C═C stretching at 1605 cm^{-1} and aromatic C−H deformation modes around 711 cm^{-1}, which were also observed by other researchers (Figure 2a).[22] The 2080 cm^{-1} peak could be arising from >C═C═O (ketone group). The FTIR spectra show a strong peak at 1408 cm^{-1}, which corresponded to the −COOH (carboxyl) symmetric stretching vibration and C−C stretching vibrations in the aromatic ring, which can be confirmed by Shao et al.[32] The peak at 1063 cm^{-1} can be related to stretching from the C−O bonds in ethers, esters, and carbonates. The peaks appearing below 1000 cm^{-1} might be related to Si−O, Si−O−Si, and Si−O−Mg stretching vibrations.[40] XRD patterns indicate the presence of calcite, dolomite, calcium silicate, and bassanite as the primary crystalline phases in eastern red cedar biochar (Figure 2b). The peaks at 26.7 and 19.5° correspond to silicon and calcium oxides, respectively.[41] The strong bands at 1408 and 871 cm^{-1} in the FTIR spectra (Figure 2a) can be assigned to calcite,[42] which is consistent with the XRD analysis of the eastern red cedar biochar. The obtained sharp peaks for biochar pyrolyzed at 450 °C indicate that the structure of calcite is well-crystallized, which is supported by the study of Al-Wabel et al.[43]

Adsorption Capacity. The removal efficiencies of tetracycline (TC), oxytetracycline (OTC), chlortetracycline (CTC), sulfadiazine (SDZ), and sulfamethazine (SMZ) were significantly affected by their initial concentrations ($p < 0.05$) (Figure 3). At the lower concentrations (100 to 300 μg L^{-1}), the removal efficiencies of TC, OTC, CTC, SDZ, and SMZ were 99.93, 96.23, 98.28, 76.4, and 78.6%, respectively, which indicates an overall antibiotic removal between 115 and 150 μg mg^{-1} of biochar. These relatively high removal rates may be due to the existence of many available binding sites on the surfaces of the eastern red cedar biochar and the formation of a large driving force during the mass transfer process.[44] When the initial concentration of the antibiotics was 900 μg L^{-1}, the mean removal efficiencies decreased to 83.52, 47.23, 64.16,

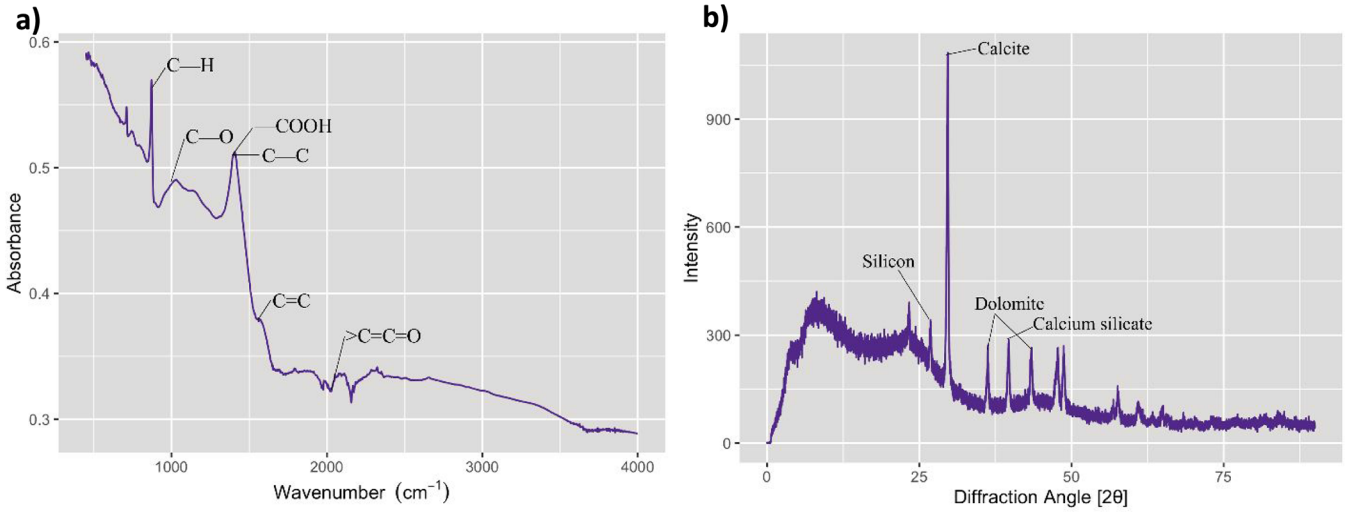

Figure 2. FTIR spectra of eastern red cedar biochar (a) and X-ray diffraction patterns of eastern red cedar biochar (b).

https://doi.org/10.1021/acsomega.4c07266
ACS Omega XXXX, XXX, XXX−XXX

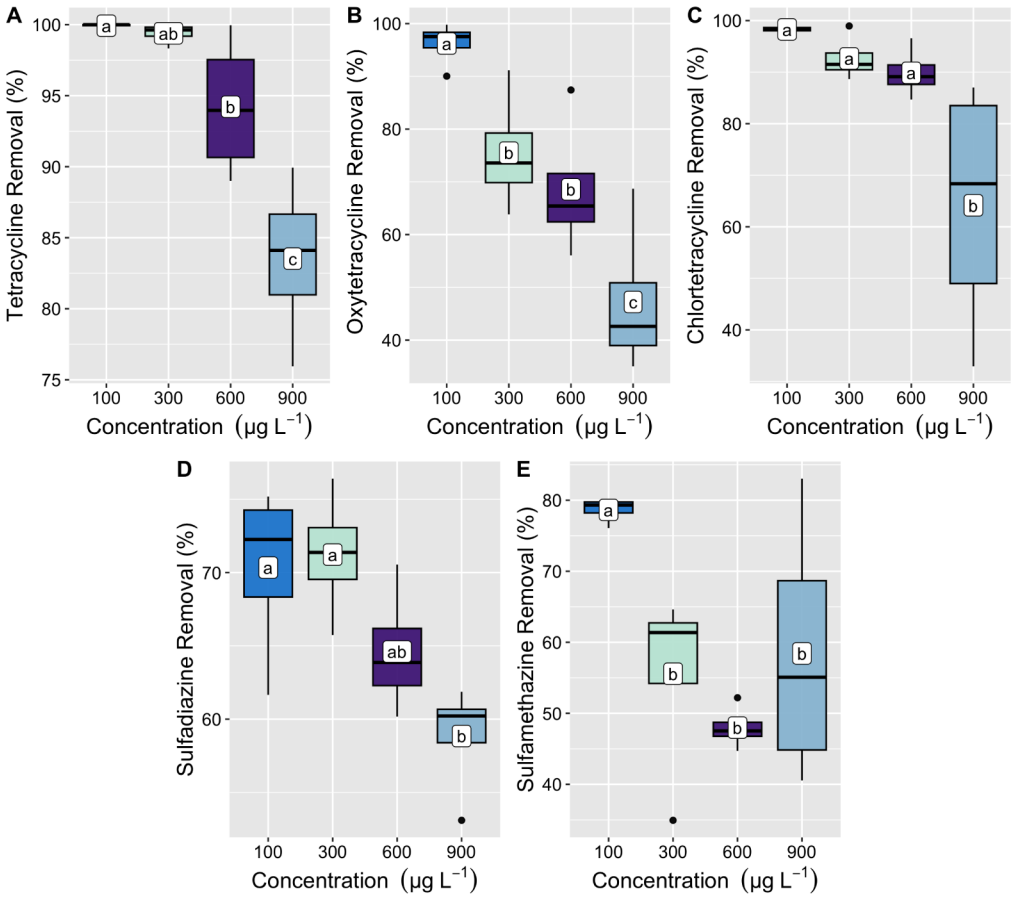

Figure 3. Removal efficiency of tetracycline (TC) (A), oxytetracycline (OTC) (B), chlortetracycline (CTC) (C), sulfadiazine (SDZ) (D), and sulfamethazine (SMZ) (E) at different concentrations (for each individual compounds). Means followed by the same letter are not statistically different according to Fisher's LSD test at 5% level. Individual points represent outliers.

69.8, and 58.4% for TC, OTC, CTC, SDZ, and SMZ, respectively, indicating antibiotic removal between 212 and 375 μg mg^{-1} of biochar. This decrease in antibiotic adsorption efficiency onto the biochar surface may be attributed to the saturation of the binding sites with higher antibiotic concentrations.[44] There are other findings in the literature in agreement with the results found in this research.[44,45] According to the results shown in Figure 3, the eastern red cedar biochar presents a diverse range of adsorption sites with different affinities and capacities. The differences in removal efficiency among replicates are likely explained by the heterogeneity of the biochar structure (Figure 1). As mentioned by Kong et al.,[46] even if the biochar is from the same source, its substantial heterogeneity results in a complex structure and diverse physical properties, thereby affecting the adsorption behavior. The biochar surface contains various functional groups such as carboxyl and carbonyl groups (Figure 2) and the distribution and availability of these groups are not uniform across the surface. This heterogeneity explains the large standard deviations observed for some concentrations. In addition, at lower concentrations, the high-affinity sites, which have stronger binding interactions with the antibiotics, are more likely to be occupied first. These sites are particularly effective in adsorbing the OTC and CTC at lower concentrations, leading to higher removal efficiencies. As the concentration of these antibiotics increases, these sites become saturated (Figure 3b,c). The remaining sites are probably of lower affinity and cannot adsorb the antibiotics as effectively, leading to a more significant drop in the removal efficiency.

In the mixture, where each class of antibiotics was mixed at the same individual concentrations (100, 300, 600, and 900 μg L^{-1}), the removal efficiencies of CTC and TC at the lowest concentrations were 96.24 and 87.01%, respectively (Figure 4a), which shows a removal of 48 μg mg^{-1} of biochar for CTC and of 43 μg mg^{-1} of biochar for TC. The removal efficiency of OTC with the initial concentration of 100 μg L^{-1} was 84.40%, showing a removal of 42 μg mg^{-1} of biochar. At the highest concentrations, the removal efficiencies declined up to 72.85% for CTC, 35.19% for OTC, and 7.78% for TC, indicating that CTC preferentially binds to the biochar surface compared to that of OTC and TC. The removal of CTC, OTC, and TC was 328, 158, and 35 μg mg^{-1} of biochar, respectively. The sorption affinity can be written in the following order: CTC > OTC > TC. The sorption affinity presumed that when antibiotics are sorbed onto the surface of biochar in competitive mode, they all share the same sorption sites. However, the degree of sorption depends on the physicochemical properties of antibiotics and biochar. As a result, the eastern red cedar biochar is capable of adsorbing a mixture of antibiotics onto its surface, which was consistent with the study of Ahmed et al.[47] on eucalyptus wood biochar. The additional chlorine atom in the chemical structure of CTC has a potential effect on the electric density of the whole molecules and enhanced polarity of CTC's functional groups, leading to stronger adsorption and increased affinity for the biochar

https://doi.org/10.1021/acsomega.4c07266
ACS Omega XXXX, XXX, XXX−XXX

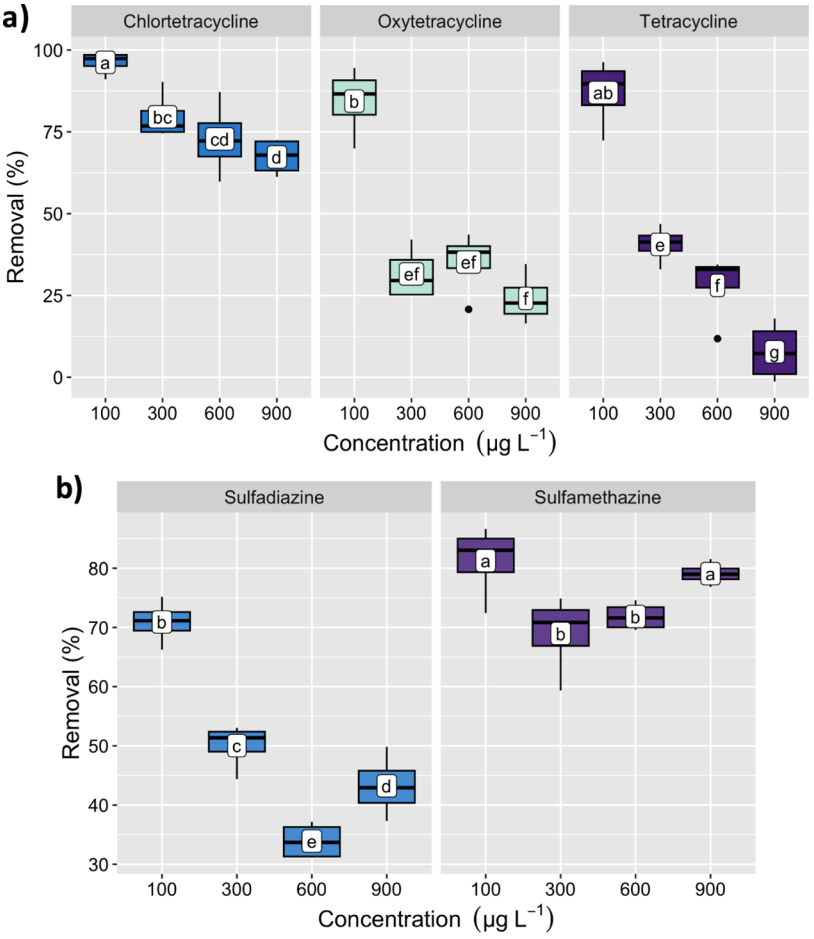

Figure 4. Removal efficiency of antibiotic mixtures: chlortetracycline (CTC), oxytetracycline (OTC), and tetracycline (TC) (a) and removal efficiency of sulfadiazine (SDZ) and sulfamethazine (SMZ) (b) at different concentrations. Means followed by the same letter are not statistically different according to Fisher's LSD test at 5% level.

compared to OTC and TC. Moreover, the eastern red cedar biochar (Figure 2a) can form hydrogen bonds with the hydroxyl groups of the hydroxyl groups of the OTC. Therefore, the adsorption capacity of the eastern red cedar biochar to the OTC is higher than the adsorption capacity of the TC.

Sulfadiazine removal efficiencies were 70.92, 50.05, 33.93, and 43.25% at concentrations of 100, 300, 600, and 900 μg L^{-1}, when mixed with SMZ (Figure 4b), indicating a removal of 35, 75, 102, and 195 μg mg^{-1} of biochar, respectively. The mean SMZ removal when combined with SDZ was 81.23% at concentrations of 100 and 900 μg L^{-1} and 71.84% at concentrations of 300 and 600 μg L^{-1}. Thus, SMZ removal for the concentrations of 100, 300, 600, and 900 μg L^{-1} were 40, 108, 215, and 366 μg mg^{-1} of biochar, respectively. Overall, SMZ showed a higher removal efficiency compared to SDZ. Similarly, Zhao et al.[48] observed that SMZ exhibited an adsorption affinity on the biochar surface that was an order of magnitude higher compared to SDZ. The varying adsorption behavior of these sulfonamides can be attributed to the different substituents connected to the amino groups (−NH−),[48] which lies in the extra dimethyl group that is present in the fourth and sixth carbon of the pyridine ring having much stronger π-electron-conjugating potential (4-amino-*N*-(4,6-dimethylpyrimidin-2-yl) benzene-sulfonamide for SMZ and 4-amino-N-(pyrimidin-2-yl) benzene-1-sulfonamide for SDZ, respectively).[49] The presence of an aromatic ring in SMZ may enhance its affinity for the hydrophobic carbonaceous structure of biochar, leading to higher adsorption capacities compared to SDZ, as previously supported by ref 50.

Overall, when the single effect was evaluated, higher adsorption efficiencies were achieved for tetracyclines compared to sulfonamides. According to Peiris et al.,[12] this increased adsorption of tetracyclines is related to their relatively high hydrophobicity compared to sulfonamides. Tetracyclines act as triprotic acids (Table 2), and their amphoteric behavior is due to the dominance of neutral and differently charged species at varying pH values. Additionally, cation bridging plays a significant role in tetracycline sorption.[12]

Tetracyclines and sulfonamides were mixed at concentrations of 600 and 300 μg L^{-1}. These concentrations were selected based on the relative proportions of tetracyclines and sulfonamides previously reported in the literature for swine wastewater.[7,26] The removal efficiency was significantly affected by the co-occurrence of the antibiotics ($p < 0.05$) (Figure 5). The highest removal efficiencies are 77.35 and 50.26% for CTC and SMZ, respectively. As previously stated, the presence of functional groups in the molecular structures of CTC and SMZ can enhance adsorption onto the surface of eastern red cedar biochar, resulting in higher removal

https://doi.org/10.1021/acsomega.4c07266
ACS Omega XXXX, XXX, XXX−XXX

Table 2. Physico-Chemical Properties of TC, OTC, CTC, SDZ, and SMZ[a]

Antibiotic	Chemical structure	Chemical formula	pKa	Log Kow
TC	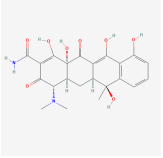	$C_{22}H_{24}N_2O_8$	$pKa_1 = 3.30$ $pKa_2 = 7.68$ $pKa_3 = 9.69$	-1.30
OTC	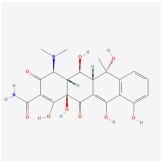	$C_{22}H_{24}N_2O_9$	$pKa_1 = 3.27$ $pKa_2 = 7.32$ $pKa_3 = 9.11$	-0.90
CTC	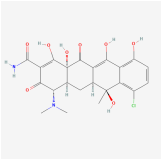	$C_{22}H_{23}ClN_2O_8$	$pKa_1 = 3.30$ $pKa_2 = 7.55$ $pKa_3 = 9.15$	-0.62
SDZ	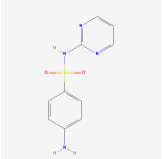	$C_{10}H_{10}N_4O_2S$	$pKa_1 = 2.0$ $pKa_2 = 6.5$	-0.90
SMZ	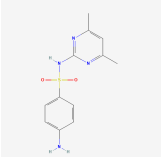	$C_{12}H_{14}N_4O_2S$	$pKa_1 = 2.65$ $pKa_2 = 7.65$	0.89

[a]Data obtained from PubChem (https://pubchem.ncbi.nlm.nih.gov/), U.S. National Library of Medicine.

efficiencies of CTC and SMZ compared with TC, OTC, and SDZ.

Adsorption Isotherms. The Langmuir and Freundlich models are two common isotherm models used to describe the adsorption of antibiotics onto solid surfaces.[51] The Langmuir isotherm model assumes that the adsorption process is a monolayer process, where each molecule adsorbs onto a specific site on the solid surface.[51] On the other hand, the Freundlich isotherm model assumes that the adsorption process is multilayer and that the adsorption sites have different energies. The value of n (slope) provides information about the adsorption mechanism. A value of n close to 1 indicates a physical adsorption process, while a value of n greater than 1 suggests a chemical adsorption process.[52]

The results for the Langmuir and Freundlich models for the tetracycline class indicate that the Langmuir model has the best fit for the experimental data with a larger correlation coefficient (Figure S1—single effect = $R^2 \geq 0.93$ and Figure 6a—mixture effect = $R^2 \geq 0.50$), suggesting that the adsorption of tetracyclines onto eastern red cedar biochar is a monolayer sorption mechanism. On the other hand, the experimental data for the sulfonamide class displayed stronger correlation with the Freundlich model, as evidenced by the higher correlation coefficients R^2 (Figure S1—single effect = $R^2 \geq 0.67$ and Figure 6b—mixture effect = $R^2 \geq 0.86$) than those in the Langmuir model.

Adsorption Mechanisms. The functional groups of tetracyclines can undergo numerous electronic coupling interactions including electrostatic interactions, $\pi-\pi$ electron-donor−acceptor, and Lewis acid−base interactions.[12] Similarly, the adsorption of sulfonamides was attributed to various mechanisms, such as hydrogen bonds, $\pi-\pi$ electron-donor−acceptor interactions, van der Waals forces, hydrophobicity, and pore-filling.[16,47] Generally, hydrogen bonding and $\pi-\pi$ electron-donor−acceptor seem to be the major mechanisms that drive the adsorptive removal of these two classes of antibiotics from aqueous solutions using carbon-based materials.[17]

On eastern red cedar biochar, hydrogen bonds played an important role in both tetracycline and sulfonamide removal due to the carboxyl group confirmed by the FTIR spectra (Figure 2a), which indicates a possible adsorption mechanism involving hydrogen bonds between the antibiotics and the carboxyl group around 1408 cm^{-1}. Phenol, amine, hydroxyl, and enone moieties of tetracyclines can form hydrogen bonding with carboxyl functional groups on biochar surfaces.[12] Likewise, the amino and amine groups from sulfonamides can interact with carboxyl and hydroxyl groups on the surface of eastern red cedar biochar through hydrogen bonding.[48]

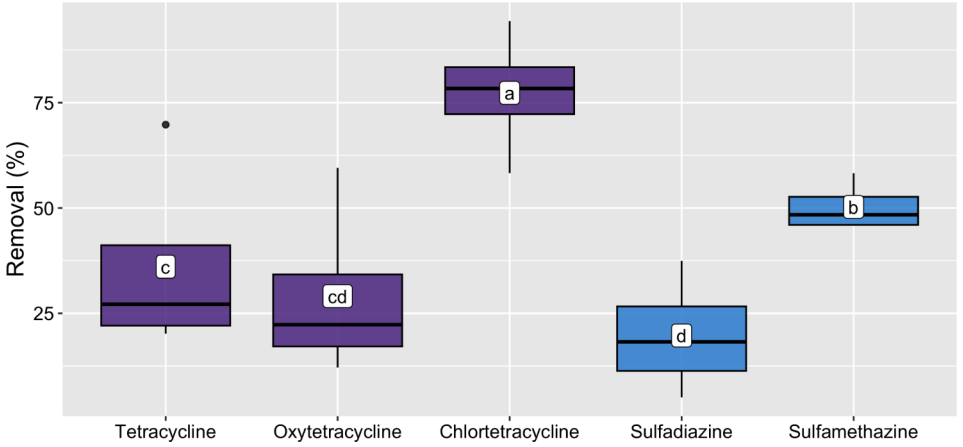

Figure 5. Removal efficiency of a mixture of tetracyclines (each at 600 $\mu g\ L^{-1}$) and sulfonamides (each at 300 $\mu g\ L^{-1}$). Means followed by the same letter are not statistically different according to Fisher's LSD test at the 5% level.

https://doi.org/10.1021/acsomega.4c07266
ACS Omega XXXX, XXX, XXX−XXX

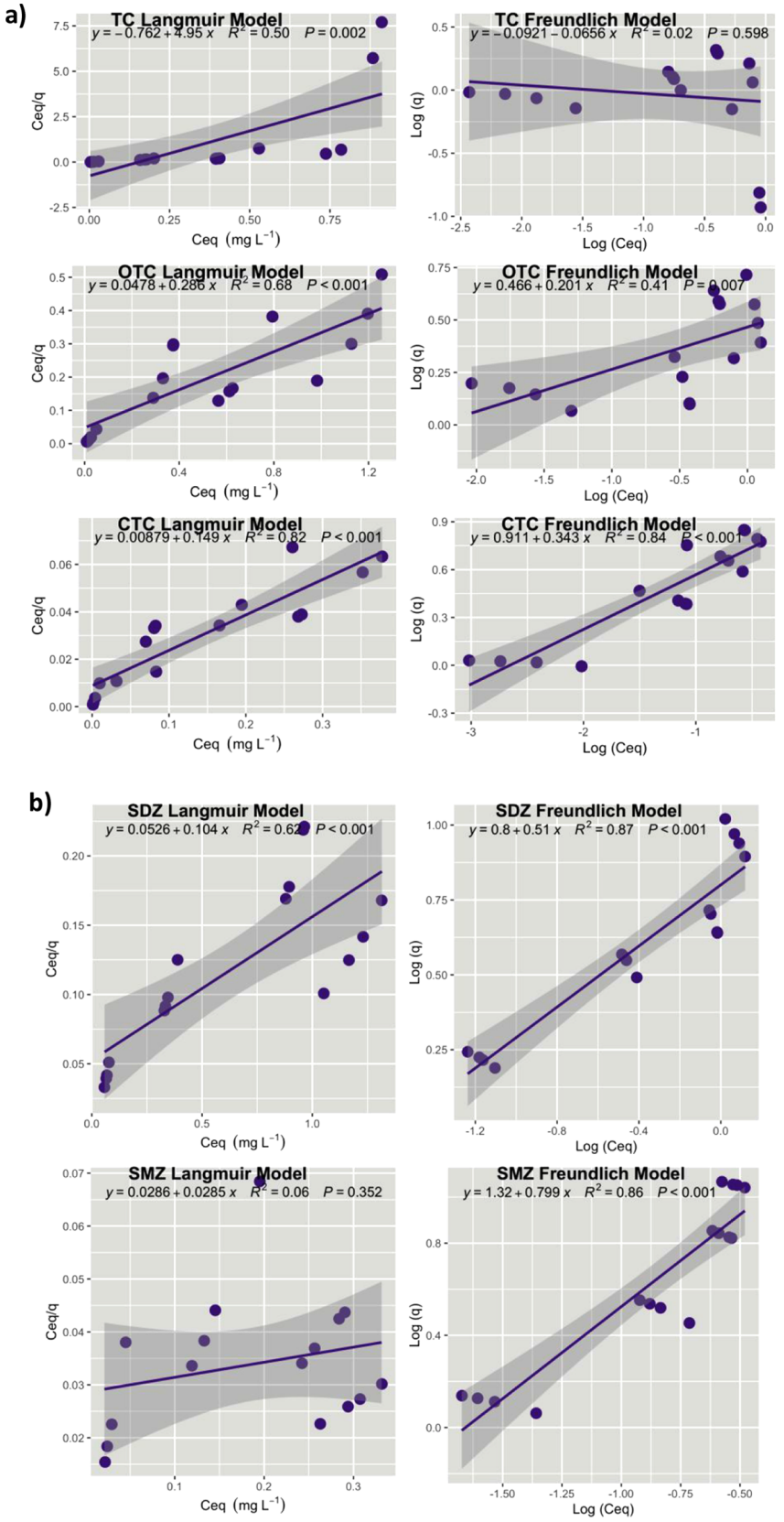

Figure 6. Langmuir and Freundlich models for the tetracycline (TC), oxytetracycline (OTC), and chlortetracycline (CTC) mixture effect (a) and Langmuir and Freundlich models for the sulfadiazine (SDZ) and sulfamethazine (SMZ) mixture effect (b).

Conjugated enone structures of tetracyclines can act as π electron acceptors considering the strong electron-withdrawing ability of the ketone group.[53] Sulfonamides can be strong π electron acceptors due to the presence of amino and aromatic groups in the molecular structure. On the other hand, the presence of a significant number of oxygen-containing

https://doi.org/10.1021/acsomega.4c07266
ACS Omega XXXX, XXX, XXX−XXX

functional groups on the eastern red cedar biochar surface (Figure 2a) indicates its potential to act as an electron donor.[54] Thus, the $\pi-\pi$ electron-donor−acceptor interaction is crucial in the adsorption process of tetracyclines and sulfonamides on eastern red cedar biochar.

Lewis acid−base interactions can also occur between Lewis acids (−OH and C═O) on the eastern red cedar biochar surface and Lewis base ($-NH_2$) on tetracyclines and sulfonamides.[12] Furthermore, since the surface area (S_{BET}) and pore volume (V_{TOT}) (Table 1) of the eastern red cedar biochar provides abundant adsorption sites (Figure 1), the favorable adsorption between the antibiotics and the biochar could be due to the pore-filling effect (SEM and BET analysis).

Nevertheless, the different adsorption efficiencies obtained for tetracyclines and sulfonamides onto biochar can be linked to particular properties of the antibiotics (Table 2). Chemical properties, specifically the octanol−water partitioning coefficient (K_{ow}) and acidity constant (pK_a), play major roles in assessing the adsorption behavior of different tetracyclines and sulfonamides. The K_{ow} is commonly used as an indicator of the adsorbate's hydrophobicity, and thus, antibiotics with low log K_{ow} are more hydrophilic.[55] The pK_a is related to the speciation of the antibiotics. Hence, the adsorption capacities of different antibiotics under the same conditions result from a combination of multiple forces.[56]

In this study, hydrophobicity can play a more important role in the sorption of SMZ and CTC on eastern red cedar biochar because these antibiotics had higher log K_{ow} than SDZ, OTC, and TC. In addition, based on the pK_{a2} values (Table 2), SDZ molecules (pK_{a2} = 6.5) were negatively charged at a pH of 7, while SMZ molecules (pK_{a2} = 7.65) existed in more neutral species. Since neutral molecules tend to be more strongly sorbed on biochar than negatively charged molecules,[56] SMZ with its more neutral species likely has a higher affinity for sorption on eastern red cedar biochar compared to SDZ with its negatively charged species at pH 7. Likewise, TC (pK_{a2} = 7.68), OTC (pK_{a2} = 7.32), and CTC (pK_{a2} = 7.55) existed in both neutral and negatively charged forms at pH 7, but OTC is more neutral as indicated by its lower pK_{a2}, which explains the higher sorption capacity when compared to TC. However, the higher sorption behavior of CTC may be explained by the enhanced polarity of CTC's functional groups due to the additional chlorine atom and thus stronger polar−polar interactions with the eastern red cedar biochar surface, which is coherent with the results found by Chen et al.[57] on aluminum oxide surfaces.

The molar ratios of O/C, H/C, and (N+O)/C represent the hydrophobicity, aromaticity, and polarity of a biochar.[58] Eastern red cedar biochar had relatively low ratios of O/C (0.20), H/C (0.03), and (N+O)/C (0.22) (Table 1), suggesting its high hydrophobicity, aromaticity, and low polarity.[56] Usually, these ratios are low with a high pyrolysis temperature, and thus, biochars produced under high temperature are highly carbonized and more hydrophobic and exhibited a highly aromatic structure.[58] However, these features are present in eastern red cedar biochar produced at a pyrolysis temperature of 450 °C (Table 1 and Figure 2a), which contributes to its adsorption efficiency.

The outcomes of this study provide a foundation for an optimistic extrapolation to real-world swine wastewater treatment scenarios. The demonstrated effectiveness of eastern red cedar biochar in removing antibiotics, even in the presence of complex chemical mixtures, suggests its potential applicability in the treatment of swine wastewater. The focus on anaerobically treated swine wastewater as a practical application can be especially valuable. By incorporating the biochar as a polishing step postanaerobic treatment, potential interferences from other wastewater constituents, such as chemical oxygen demand (COD) and solids, can be minimized. Anaerobic treatment processes typically target and remove organic matter and solids, creating a more controlled environment for biochar to specifically address antibiotic residues. This approach aligns with a cost-effective and environmentally friendly wastewater treatment strategy, further underscoring the versatility and feasibility of utilizing eastern red cedar biochar in addressing antibiotic contamination in swine wastewater.

CONCLUSION

In summary, the adsorptive removal of tetracyclines (TC, OTC, and CTC) and sulfonamides (SDZ and SMZ) from swine wastewater by eastern red cedar biochar was investigated at four different antibiotic concentrations. At the lowest concentrations (100 to 300 $\mu g\ L^{-1}$), the removal efficiencies of TC, OTC, CTC, SDZ, and SMZ were 99.93, 96.23, 98.28, 76.4, and 78.6%, respectively. At higher concentrations (600 to 900 $\mu g\ L^{-1}$), the removal efficiencies decreased to 83.52, 47.23, 64.16, 69.8, and 58.4% for TC, OTC, CTC, SDZ, and SMZ. When antibiotics were combined, the eastern red cedar biochar exhibited stronger adsorption capacity for CTC and SMZ compared to TC, OTC, and SDZ. The adsorption capacity and mechanism can be significantly influenced by the chemical properties of each antibiotic and the surface properties of the biochar. Sorption of tetracyclines was described by the Langmuir adsorption isotherm model adequately, indicating that it is a monolayer sorption on the biochar surface. On the other hand, sorption data of sulfonamides were better fitted to the Freundlich model, implying that electrostatic interactions existed in the midst of heterogeneous sites on eastern red cedar biochar. Mostly, the major adsorption mechanisms driving the removal of both sulfonamides and tetracyclines from the aqueous solution are hydrogen bonding and $\pi-\pi$ electron-donor−acceptor interactions, whereas Lewis base−acid interactions and pore-filling may be auxiliary sorption mechanisms. The results highlighted that eastern red cedar biochar may be a promising adsorbent to be used for practical applications, mitigating antibiotic residues from swine wastewater in a cost-effective and environmentally friendly manner due to its relatively low pyrolysis temperature (450 °C) and beneficial use of an invasive species.

ASSOCIATED CONTENT

Supporting Information

The Supporting Information is available free of charge at https://pubs.acs.org/doi/10.1021/acsomega.4c07266.

Langmuir and Freundlich models for tetracycline (TC), oxytetracycline (OTC), chlortetracycline (CTC), sulfadiazine (SDZ), and sulfamethazine (SMZ) as single effects (PDF)

AUTHOR INFORMATION

Corresponding Author

Jessica de Oliveira Demarco − *Department of Biological and Agricultural Engineering, Kansas State University,*

https://doi.org/10.1021/acsomega.4c07266
ACS Omega XXXX, XXX, XXX−XXX

Manhattan, Kansas 66506, United States; orcid.org/0000-0001-5255-1873; Email: demarcoj@ksu.edu

Authors

Stacy L. Hutchinson − *Department of Biological and Agricultural Engineering, Kansas State University, Manhattan, Kansas 66506, United States*

Prathap Parameswaran − *Department of Civil Engineering, Kansas State University, Manhattan, Kansas 66506, United States*

Ganga Hettiarachchi − *Department of Agronomy, Kansas State University, Manhattan, Kansas 66506, United States;* orcid.org/0000-0002-6669-2885

Trisha Moore − *Department of Biological and Agricultural Engineering, Kansas State University, Manhattan, Kansas 66506, United States*

Complete contact information is available at: https://pubs.acs.org/10.1021/acsomega.4c07266

Notes

The authors declare no competing financial interest.

■ ACKNOWLEDGMENTS

This research was supported by the U.S. Department of Energy [DE-EE0009504]. The biochar was supplied by Jeffery Neel (Blue Earth, LLC).

■ REFERENCES

(1) Cheng, D.; Ngo, H. H.; Guo, W.; Chang, S. W.; Nguyen, D. D.; Liu, Y.; Wei, Q.; Wei, D. A critical review on antibiotics and hormones in swine wastewater: Water pollution problems and control approaches. *J. Hazard. Mater.* **2020**, *387*, 121682.

(2) Kasimanickam, V.; Kasimanickam, M.; Kasimanickam, R. Antibiotics Use in Food Animal Production: Escalation of Antimicrobial Resistance: Where Are We Now in Combating AMR? *Med. Sci.* **2021**, *9* (1), 14.

(3) Spielmeyer, A. Occurrence and fate of antibiotics in manure during manure treatments: A short review. *Sustainable Chem. Pharm.* **2018**, *9* (2018), 76−86.

(4) Xu, R.; Wu, Z.; Zhou, Z.; Meng, F. Removal of sulfadiazine and tetracycline in membrane bioreactors: Linking pathway to microbial community shift. *Environ. Technol.* **2019**, *40* (2), 134−143.

(5) Zhang, Q. Q.; Ying, G. G.; Pan, C. G.; Liu, Y. S.; Zhao, J. L. Comprehensive evaluation of antibiotics emission and fate in the river basins of China: Source analysis, multimedia modeling, and linkage to bacterial resistance. *Environ. Sci. Technol.* **2015**, *49* (11), 6772−6782.

(6) Zhang, G.; Liu, X.; Sun, K.; He, F.; Zhao, Y.; Lin, C. Competitive Sorption of Metsulfuron-Methyl and Tetracycline on Corn Straw Biochars. *J. Environ. Qual.* **2012**, *41* (6), 1906−1915.

(7) Wan, Y. P.; Liu, Z. H.; Liu, Y. Veterinary antibiotics in swine and cattle wastewaters of China and the United States: Features and differences. *Water Environ. Res.* **2021**, *93* (9), 1516−1529.

(8) Udebuani, A. C.; Pereao, O.; Akharame, M. O.; Fatoki, O. S.; Opeolu, B. O. The potential ecological risk of veterinary pharmaceuticals from swine wastewater on freshwater aquatic environment. *Water Environ. Res.* **2023**, *95* (1), No. e10833.

(9) Li, X.; Liu, C.; Chen, Y.; Huang, H.; Ren, T. Antibiotic residues in liquid manure from swine feedlot and their effects on nearby groundwater in regions of North China. *Environ. Sci. Pollut. Res.* **2018**, *25*, 11565−11575.

(10) Chen, J.; Liu, Y.-S.; Zhang, J.-N.; Yang, Y.-Q.; Hu, L.-X.; Yang, Y.-Y.; Zhao, J. L.; Chen, F.-R.; Ying, G.-G. Removal of antibiotics from piggery wastewater by biological aerated filter system: Treatment efficiency and biodegradation kinetics. *Bioresour. Technol.* **2017**, *238*, 70−77.

(11) Li, R.; Wang, J. J.; Zhou, B.; Zhang, Z.; Liu, S.; Lei, S.; Xiao, R. Simultaneous capture removal of phosphate, ammonium and organic substances by MgO impregnated biochar and its potential use in swine wastewater treatment. *J. Cleaner Prod.* **2017**, *147* (2017), 96−107.

(12) Peiris, C.; Gunatilake, S. R.; Mlsna, T. E.; Mohan, D.; Vithanage, M. Biochar based removal of antibiotic sulfonamides and tetracyclines in aquatic environments: A critical review. *Bioresour. Technol.* **2017**, *246*, 150−159.

(13) Chaukura, N.; Gwenzi, W.; Tavengwa, N.; Manyuchi, M. M. Biosorbents for the removal of synthetic organics and emerging pollutants: Opportunities and challenges for developing countries. *Environ. Dev.* **2016**, *19* (2016), 84−89.

(14) Gwenzi, W.; Chaukura, N.; Noubactep, C.; Mukome, F. N. Biochar-based water treatment systems as a potential low-cost and sustainable technology for clean water provision. *J. Environ. Manage.* **2017**, *197*, 732−749.

(15) Supraja, K. V.; Kachroo, H.; Viswanathan, G.; Verma, V. K.; Behera, B.; Doddapaneni, T. R. K. C.; Kaushal, P.; Ahammad, S. Z.; Singh, V.; Awasthi, M. K.; et al. Biochar production and its environmental applications: Recent developments and machine learning insights. *Bioresour. Technol.* **2023**, *387*, 129634.

(16) Zhang, X.; Zhang, Y.; Ngo, H. H.; Guo, W.; Wen, H.; Zhang, D.; Li, C.; Qi, L. Characterization and sulfonamide antibiotics adsorption capacity of spent coffee grounds based biochar and hydrochar. *Sci. Total Environ.* **2020**, *716*, 137015.

(17) Biswal, B. K.; Balasubramanian, R. Adsorptive removal of sulfonamides, tetracyclines and quinolones from wastewater and water using carbon-based materials: Recent developments and future directions. *J. Cleaner Prod.* **2022**, *349*, 131421.

(18) Hu, J.; Liu, F.; Shan, Y.; Huang, Z.; Gao, J.; Jiao, W. Enhanced Adsorption of Sulfonamides by Attapulgite-Doped Biochar Prepared with Calcination. *Molecules* **2022**, *27* (22), 8076.

(19) Homagain, K.; Shahi, C.; Luckai, N.; Sharma, M. Life cycle cost and economic assessment of biochar-based bioenergy production and biochar land application in Northwestern Ontario, Canada. *For. Ecosyst.* **2016**, *3*, 1−10.

(20) Vuppaladadiyam, A. K.; Vuppaladadiyam, S. S. V.; Sahoo, A.; Murugavelh, S.; Anthony, E.; Bhaskar, T.; Zheng, Y.; Zhao, M.; Duan, H.; Zhao, Y.; et al. Bio-oil and biochar from the pyrolytic conversion of biomass: A current and future perspective on the trade-off between economic, environmental, and technical indicators. *Sci. Total Environ.* **2023**, *857*, 159155.

(21) Amoah-Antwi, C.; Kwiatkowska-Malina, J.; Thornton, S. F.; Fenton, O.; Malina, G.; Szara, E. Restoration of soil quality using biochar and brown coal waste: A review. *Sci. Total Environ.* **2020**, *722*, 137852.

(22) Liu, Y.; He, Z.; Uchimiya, M. Comparison of biochar formation from various agricultural by-products using FTIR spectroscopy. *Mod. Appl. Sci.* **2014**, *9* (4), 246.

(23) Vaughn, S. F.; Byars, J. A.; Jackson, M. A.; Peterson, S. C.; Eller, F. J. Tomato seed germination and transplant growth in a commercial potting substrate amended with nutrient-preconditioned eastern red cedar (*Juniperus virginiana* L.) wood biochar. *Sci. Hortic.* **2021**, *280*, 109947.

(24) Jeffries, K.; Mishra, B.; Russell, A.; Joshi, O. Exploring Opinions for Using Prescribed Fire to Control Eastern Redcedar (*Juniperus virginiana*) Encroachment in the Southern Great Plains, United States. *Rangel. Ecol. Manag.* **2023**, *86*, 73−79.

(25) Vaughn, S. F.; Winkler-Moser, J. K.; Berhow, M. A.; Byars, J. A.; Liu, S. X.; Jackson, M. A.; Peterson, S. C.; Eller, F. J. An odor-reducing, low dust-forming, clumping cat litter produced from Eastern red cedar (*Juniperus virginiana* L.) wood fibers and biochar1. *Ind. Crops Prod.* **2020**, *147*, 112224.

(26) Cheng, D.; Ngo, H. H.; Guo, W.; Chang, S. W.; Nguyen, D. D.; Liu, Y.; Shan, X.; Nghiem, L. D.; Nguyen, L. N. Removal process of antibiotics during anaerobic treatment of swine wastewater. *Bioresour. Technol.* **2020**, *300*, 122707.

(27) Harb, M.; Zarei-Baygi, A.; Wang, P.; Sawaya, C. B.; McCurry, D. L.; Stadler, L. B.; Smith, A. L. Antibiotic transformation in an anaerobic membrane bioreactor linked to membrane biofilm microbial activity. *Environ. Res.* **2021**, *200*, 111456.
(28) Liu, W.; Xia, R.; Ding, X.; Cui, W.; Li, T.; Li, G.; Luo, W. Impacts of nano-zero-valent iron on antibiotic removal by anaerobic membrane bioreactor for swine wastewater treatment. *J. Membr. Sci.* **2022**, *659*, 120762.
(29) Ashiq, A.; Walpita, J.; Vithanage, M. Functionalizing non-smectic clay via methoxy-modification for enhanced removal and recovery of oxytetracycline from aqueous media. *Chemosphere* **2021**, *276*, 130079.
(30) Alabbad, E. A.; Bashir, S.; Liu, J. L. Efficient removal of direct yellow dye using chitosan crosslinked isovanillin derivative biopolymer utilizing triboelectric energy produced from homogeneous catalysis. *Catal. Today* **2022**, *400*, 132−145.
(31) R Core Team *R: A Language and Environment for Statistical Computing*. R Foundation for Statistical Computing, Vienna, Austria: 2021.
(32) Shao, F.; Zhang, X.; Sun, X.; Shang, J. Antibiotic removal by activated biochar: Performance, isotherm, and kinetic studies. *J. Dispersion Sci. Technol.* **2021**, *42* (9), 1274−1285.
(33) Sharma, T.; Ratner, A. Analysis and characterization of metallic nodules on biochar from single-stage downdraft gasification. *Processes* **2021**, *9* (3), 533.
(34) Zhao, J.; Liang, G.; Zhang, X.; Cai, X.; Li, R.; Xie, X.; Wang, Z. Coating magnetic biochar with humic acid for high efficient removal of fluoroquinolone antibiotics in water. *Sci. Total Environ.* **2019**, *688*, 1205−1215.
(35) Yargicoglu, E. N.; Sadasivam, B. Y.; Reddy, K. R.; Spokas, K. Physical and chemical characterization of waste wood derived biochars. *Waste Manage.* **2015**, *36*, 256−268.
(36) Liu, Q.; Wen, Y.; Zhong, M.; Hu, H.; Jin, L. Insight into pyrolysis behaviors of cedar under different atmospheres via a fixed-bed reactor. *Fuel* **2024**, *368*, 131607.
(37) Zhao, L.; Cao, X.; Mašek, O.; Zimmerman, A. Heterogeneity of biochar properties as a function of feedstock sources and production temperatures. *J. Hazard. Mater.* **2013**, *256*, 1−9.
(38) Suliman, W.; Harsh, J. B.; Abu-Lail, N. I.; Fortuna, A. M.; Dallmeyer, I.; Garcia-Perez, M. Influence of feedstock source and pyrolysis temperature on biochar bulk and surface properties. *Biomass Bioenergy* **2016**, *84*, 37−48.
(39) Elnour, A. Y.; Alghyamah, A. A.; Shaikh, H. M.; Poulose, A. M.; Al-Zahrani, S. M.; Anis, A.; Al-Wabel, M. I. Effect of pyrolysis temperature on biochar microstructural evolution, physicochemical characteristics, and its influence on biochar/polypropylene composites. *Appl. Sci.* **2019**, *9* (6), 1149.
(40) Premarathna, K. S. D.; Rajapaksha, A. U.; Adassoriya, N.; Sarkar, B.; Sirimuthu, N. M.; Cooray, A.; Ok, Y. S.; Vithanage, M. Clay-biochar composites for sorptive removal of tetracycline antibiotic in aqueous media. *J. Environ. Manage.* **2019**, *238*, 315−322.
(41) Qian, K.; Kumar, A.; Bellmer, D.; Yuan, W.; Wang, D.; Eastman, M. A. Physical properties and reactivity of char obtained from downdraft gasification of sorghum and eastern red cedar. *Fuel* **2015**, *143*, 383−389.
(42) Singh, B.; Fang, Y.; Johnston, C. T. A fourier-transform infrared study of biochar aging in soils. *Soil Sci. Soc. Am. J.* **2016**, *80* (3), 613−622.
(43) Al-Wabel, M. I.; Al-Omran, A.; El-Naggar, A. H.; Nadeem, M.; Usman, A. R. Pyrolysis temperature induced changes in characteristics and chemical composition of biochar produced from conocarpus wastes. *Bioresour. Technol.* **2013**, *131*, 374−379.
(44) Hao, D.; Chen, Y.; Zhang, Y.; You, N. Nanocomposites of zero-valent iron@ biochar derived from agricultural wastes for adsorptive removal of tetracyclines. *Chemosphere* **2021**, *284*, 131342.
(45) Shan, D.; Deng, S.; Zhao, T.; Wang, B.; Wang, Y.; Huang, J.; Yu, G.; Winglee, J.; Wiesner, M. R. Preparation of ultrafine magnetic biochar and activated carbon for pharmaceutical adsorption and subsequent degradation by ball milling. *J. Hazard. Mater.* **2016**, *305*, 156−163.
(46) Kong, W.; Zhang, M.; Liu, Y.; Gou, J.; Wei, Q.; Shen, B. Physico-chemical characteristics and the adsorption of ammonium of biochar pyrolyzed from distilled spirit lees, tobacco fine and Chinese medicine residues. *J. Anal. Appl. Pyrolysis* **2021**, *156*, 105148.
(47) Ahmed, M. B.; Zhou, J. L.; Ngo, H. H.; Guo, W.; Johir, M. A. H.; Belhaj, D. Competitive sorption affinity of sulfonamides and chloramphenicol antibiotics toward functionalized biochar for water and wastewater treatment. *Bioresour. Technol.* **2017**, *238*, 306−312.
(48) Zhao, H.; Liu, X.; Cao, Z.; Zhan, Y.; Shi, X.; Yang, Y.; Zhou, J.; Xu, J. Adsorption behavior and mechanism of chloramphenicols, sulfonamides, and non-antibiotic pharmaceuticals on multi-walled carbon nanotubes. *J. Hazard. Mater.* **2016**, *310*, 235−245.
(49) Ovung, A.; Bhattacharyya, J. Sulfonamide drugs: Structure, antibacterial property, toxicity, and biophysical interactions. *Biophys. Rev.* **2021**, *13* (2), 259−272.
(50) Serna-Carrizales, J. C.; Collins-Martínez, V. H.; Flórez, E.; Gomez-Duran, C. F.; Palestino, G.; Ocampo-Pérez, R. Adsorption of sulfamethoxazole, sulfadiazine and sulfametazine in single and ternary systems on activated carbon. Experimental and DFT computations. *J. Mol. Liq.* **2021**, *324*, 114740.
(51) Liu, L.; Luo, X. B.; Ding, L.; Luo, S. L. 4 - Application of Nanotechnology in the Removal of Heavy Metal From Water. In *Nanomaterials for the Removal of Pollutants and Resource Reutilization*; Elsevier, 2019, pp. 83−147.
(52) Kalam, S.; Abu-Khamsin, S. A.; Kamal, M. S.; Patil, S. Surfactant adsorption isotherms: A review. *ACS Omega* **2021**, *6* (48), 32342−32348.
(53) Jing, X. R.; Wang, Y. Y.; Liu, W. J.; Wang, Y. K.; Jiang, H. Enhanced adsorption performance of tetracycline in aqueous solutions by methanol-modified biochar. *J. Chem. Eng.* **2014**, *248*, 168−174.
(54) Geng, X.; Lv, S.; Yang, J.; Cui, S.; Zhao, Z. Carboxyl-functionalized biochar derived from walnut shells with enhanced aqueous adsorption of sulfonamide antibiotics. *J. Environ. Manage.* **2021**, *280*, 111749.
(55) Harrower, J.; McNaughtan, M.; Hunter, C.; Hough, R.; Zhang, Z.; Helwig, K. Chemical fate and partitioning behavior of antibiotics in the aquatic environment—a review. *Environ. Toxicol. Chem.* **2021**, *40* (12), 3275−3298.
(56) Zhang, X.; Wang, Y.; Cai, J.; Wilson, K.; Lee, A. F. Bio/hydrochar sorbents for environmental remediation. *Energy Environ. Mater.* **2020**, *3* (4), 453−468.
(57) Chen, W. R.; Huang, C. H. Adsorption and transformation of tetracycline antibiotics with aluminum oxide. *Chemosphere* **2010**, *79* (8), 779−785.
(58) Rajapaksha, A. U.; Vithanage, M.; Zhang, M.; Ahmad, M.; Mohan, D.; Chang, S. X.; Ok, Y. S. Pyrolysis condition affected sulfamethazine sorption by tea waste biochars. *Bioresour. Technol.* **2014**, *166*, 303−308.

https://doi.org/10.1021/acsomega.4c07266
ACS Omega XXXX, XXX, XXX−XXX